

Please cite as:

van de Waterbeemd, M., Lössl, P., Gautier, V., Marino, F., Yamashita, M., Conti, E., Scholten, A. and Heck, A. J. R. (2014), Simultaneous Assessment of Kinetic, Site-Specific, and Structural Aspects of Enzymatic Protein Phosphorylation. *Angew. Chem. Int. Ed.*, 53: 9660–9664.

doi: 10.1002/anie.201404637

Simultaneous Assessment of Kinetic, Site-Specific and Structural Aspects of Enzymatic Protein Phosphorylation**

Michiel van de Waterbeemd, Philip Lössl, Violette Gautier, Fabio Marino, Masami Yamashita, Elena Conti, Arjen Scholten, Albert J.R. Heck*

Abstract: Protein phosphorylation is a widespread process forming the mechanistic basis of cellular signaling. Up to now, its different aspects, e.g. site-specificity, kinetics, role of co-factors and structure-function relationships are typically investigated by multiple techniques, incompatible with one another. The approach introduced here maximizes the amount of information gained on protein (complex) phosphorylation while minimizing sample handling. Using high-resolution native mass spectrometry on intact protein (assemblies) up to 150 kDa we track the sequential incorporation of phosphate groups and map their localization by peptide LC-MS/MS. On two model systems, the protein kinase G and the Aurora kinase A/Bora interplay, we demonstrate the simultaneous monitoring of various aspects of the phosphorylation process, namely the effect of different cofactors on PKG auto-phosphorylation and the interaction of AurA and Bora as both enzyme/substrate pair and physical binding partners.

Phosphorylation of proteins, where phosphotransferases (kinases) transfer inorganic phosphate from adenosine-5'-triphosphate (ATP) to substrate amino acids (mainly threonine, serine and tyrosine), is a universal process in biological systems. It affects the activity, conformation, localization, oligomeric state and/or binding repertoire of the substrate proteins and forms the basis of ubiquitous cellular signaling events.^[1] The global high-throughput analysis of dynamic protein phosphorylation (phosphoproteomics) has become feasible and datasets with over ten thousand phosphorylation sites per experiment have been reported.^[2] However, more in-depth, diverse and multidimensional low-throughput analyses are required to fully understand the functional implications of a protein phosphorylation event. Presently, protein

phosphorylation is often investigated at separate levels by using disparate methods that require different sample preparation steps or even specific engineering of the proteins. First, at the amino acid sequence level, phosphosite-specific antibodies^[3] or mass spectrometric proteomics approaches can be used to gather site-specific information, for example sequence motifs recognized by a kinase and possible cross-talk between different modified sites.^[4] Secondly, kinetic biochemical analyses, e. g. radiometric or fluorescence/luminescence assays, can provide information on the reaction rates of each enzyme-substrate pair, requirements of co-factors or the influence of environmental conditions on kinase activation, deactivation and inhibition.^[5] Thirdly, a range of structural effects of the phosphorylation event can be interrogated, for example changes in conformation, oligomeric state, and protein complex formation or dissociation,^[6] by using structural biology methods such as nuclear magnetic resonance spectroscopy (NMR), X-ray crystallography and electron microscopy.^[7]

Ideally, a single method would allow the simultaneous analysis of protein phosphorylation at all these three levels. Mass spectrometric analysis of proteins and protein complexes under non-denaturing conditions (native mass spectrometry^[8]) offers the potential to provide information at both the structural and the kinetic level, as phosphate incorporation can be identified by a characteristic mass shift of nominally 80 Da and the non-denaturing setting enables monitoring of changes within non-covalently bound protein assemblies. However, as phosphate incorporation in proteins and protein complexes only causes a minimal mass shift (<0.5%), the mass resolution needs to be sufficient for the detailed recording of sequential phosphorylation events. In 2012 we introduced an Orbitrap mass analyzer with extended mass range^[9] that provides very high mass resolution, allowing for example to resolve complex glycosylation profiles on antibodies.^[10] Making use of this novel instrument we designed an approach to maximize the amount of information that can be derived from protein phosphorylation while minimizing sample preparation, consumption, and analysis time. High resolution mass spectrometric analysis of proteins and protein complexes facilitates baseline resolution of differentially phosphorylated proteoforms, enabling us to count the number of sequentially incorporated phosphates, relatively quantify all occurring phospho-isoforms and visualize transitions on the level of non-covalent protein interactions. To obtain information on amino acid sequence level as well, we further extended this method and subjected the phosphorylated proteins, originally generated for the native MS analysis, also to bottom-up liquid-chromatography tandem mass spectrometry (LC-MS/MS), thereby acquiring extensive sequential and site specific information of the phosphorylation event. This generic workflow (Figure 1) thus provides the opportunity to obtain data on all described facets of protein phosphorylation.

[*] Michiel van de Waterbeemd,^[†] Philip Lössl,^[†] Violette Gautier, Fabio Marino, Arjen Scholten, Albert J.R. Heck
Biomolecular Mass Spectrometry and Proteomics, Bijvoet Center for Biomolecular Research and Utrecht Institute for Pharmaceutical Sciences and Netherlands Proteomics Center, Utrecht University, Padualaan 8, 3584 CH Utrecht, The Netherlands.
E-Mail: a.j.r.heck@uu.nl

Masami Yamashita, Elena Conti
Department of Structural Cell Biology, Max Planck Institute of Biochemistry, Am Klopferspitz 18, 82152 Martinsried, Germany.

[†] These authors contributed equally to this work.

[**] This work was supported by the Netherlands Proteomics Center, FOM institute (projectruimte grant 12PR3033-2), the ManiFold project (grant agreement number 317371) and the PRIME-XS project (grant agreement number 262067), both funded by the European Union 7th Framework Programme.

Supporting information for this article is available on the WWW under <http://dx.doi.org/10.1002/anie.201xxxxx>.

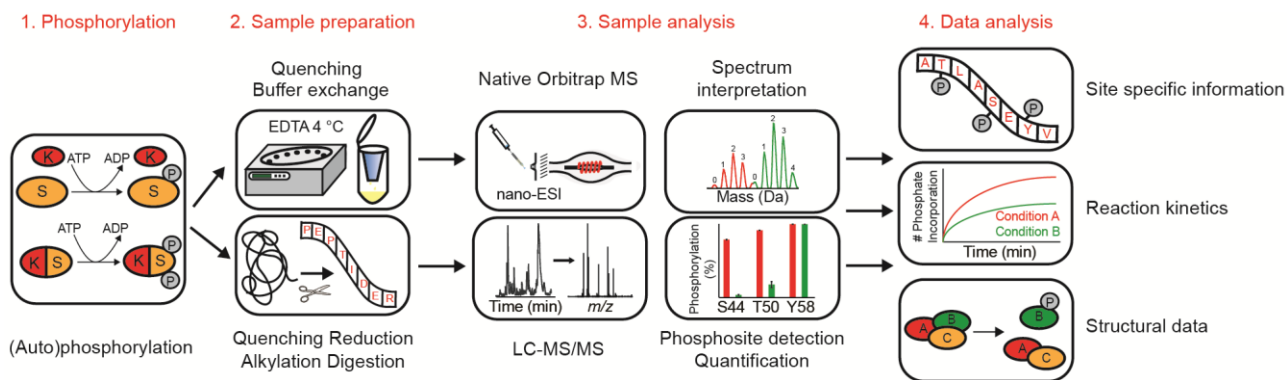


Figure 1. Overview of the all-inclusive MS-based method to investigate protein phosphorylation. (1) A kinase (K) and its substrate (S) are incubated with Mg^{2+} , ATP and other essential cofactors to initiate (auto)phosphorylation. (2 and 3) Samples are split and prepared for high-resolution native MS analysis on the Orbitrap (top) or bottom-up LC-MS/MS analysis (bottom). (4) Data analysis provides information at the sequence, kinetic and structural level.

We apply our approach on two challenging and interesting systems; the cGMP-dependent protein kinase G (PKG), that phosphorylates residues from its own N-terminus upon cGMP (cyclic guanosine monophosphate) or cAMP (cyclic adenosine monophosphate) binding-induced activation,^[11] and the Aurora kinase A (AurA), that phosphorylates its interaction partner Protein aurora borealis (Bora).^[12] PKG is highly expressed in all types of smooth muscle cells, platelets and certain areas of the brain, playing an important role in synaptic activity and smooth muscle contraction.^[13] The interplay of Aurora kinase A and Bora is critical for eukaryotic cells to enter mitosis as they form a protein complex and cooperatively activate polo-like kinase 1.^[12] Here, we demonstrate the potential of this integrated mass spectrometric approach to simultaneously characterize site-specific, kinetic and structural aspects of these enzymatic phosphorylation reactions.

Initially, we probed untreated PKG by native MS (Figure 2a). Based on the mass-to-charge ratios (m/z) of adjacent peaks of the charge state envelope^[14] the accurate molecular weight of the kinase is calculated to be 152817.6 Da, corresponding with the expected mass of homodimeric PKG (Supplementary Table 1). Figure 2b shows that, as a result of the purification procedure, up to 2 cAMP molecules are intrinsically attached to PKG and the loading state is increased to 4 cAMP molecules upon incubation with 30 μ M cAMP (species I-V). In presence of 10 μ M cGMP, 3-4 cGMP molecules are found to bind non-covalently to PKG (species VI-VII), displacing all cAMP molecules, as evidenced by the experimentally determined mass, and reflecting PKG's known higher affinity to cGMP.^[15] Owing to the high resolving power of the Orbitrap, we can not only count the number of cyclic nucleotide molecules bound to PKG but also distinguish between the differentially phosphorylated isoforms of each protein/co-factor complex, demonstrating that the predominant proteoform of the PKG dimer has consistently 2 phosphates incorporated (Figure 2b). To investigate how cyclic nucleotide binding triggers PKG auto-phosphorylation, we incubated PKG with cAMP or cGMP in presence of Mg^{2+} and ATP and monitored the reaction over time with native MS. We acquired the PKG spectra with a mass resolution of \sim 6000 (full width at half maximum), facilitating baseline resolution of all different phospho-isoforms. Progressive binding of phosphate is illustrated by a continuous signal shift to higher m/z . We detect up to 13 or 6 phosphorylations on the PKG dimer in presence of cAMP or cGMP, respectively (Figure 2c). In total, we identify 56 proteoforms of PKG/cyclic nucleotide complexes (Supplementary Tables 1 and 2). Deconvolution of the

mass spectra to zero charge state allowed us to calculate the weighted average number of phosphate incorporations based on the relative signal intensities (Figure 2d). Evidently, the maximum number of phosphorylations on PKG/cAMP complexes is substantially higher than on PKG/cGMP complexes, as schematically depicted in Figure 2e. This finding is confirmed by quantitative bottom-up LC-MS/MS analysis of the sample representing the final time point (Figure 2f). In line with the native MS data we identify 3 highly phosphorylated sites per PKG monomer, when PKG interacted with cGMP, but 6 highly phosphorylated sites for the PKG/cAMP complex, all in the vicinity of the N-terminus. In compliance with the identification of 2 phosphorylations on purified PKG dimer, residue Thr516 (located on the activation loop) is shown to be fully phosphorylated also without Mg^{2+} -ATP incubation.

Next, we aimed to apply this workflow to investigate the interaction of the kinase domain of Aurora kinase A (32.9 kDa) and an N-terminal fragment of Bora (17.5 kDa). Native MS analysis of AurA and Bora (molar ratio 1:2) confirms the formation of a 1:1 complex after incubation with Mg^{2+} and ATP (Figure 3a), as previously reported by Hutterer et al.^[12b] In contrast to the results of co-immunoprecipitation studies with full-length Bora and AurA,^[16] we observe complex formation also in absence of Mg^{2+} -ATP, i.e. with unphosphorylated Bora. Nevertheless, the complex forms more readily following incubation with Mg^{2+} -ATP, indicating a higher AurA binding affinity of phosphorylated Bora. Since we obtained baseline resolution of all phospho-isoforms of AurA, Bora and the 1:1 complex with our native MS setup we were able to study the enzyme-substrate relationship of AurA and Bora in a time-course experiment. Human AurA, purified from *E. coli* following over-expression, is found to bear up to 7 phosphate groups. Quantitative bottom-up LC-MS/MS experiments reveal 100% phosphorylation on Thr288, a modification being essential for full enzymatic activity of AurA^[17] (Figure S1). Incubating AurA with Mg^{2+} and ATP does not change its phosphorylation state (Figure 3b). AurA is, however, catalytically active as illustrated in Figure 3c. Bora as well as the AurA/Bora complex become increasingly phosphorylated following incubation with Mg^{2+} -ATP. In the control, where no Mg^{2+} -ATP was added, only unphosphorylated Bora is detected and the phospho-isoform distribution of the complex resembles the phosphorylation state of AurA. After 180 min reaction time, up to 6 phosphorylations are detected on Bora and the complex exhibits a maximum of 10 phosphate incorporations. Calculating the weighted average number of phosphorylations confirms that both complex and Bora follow the

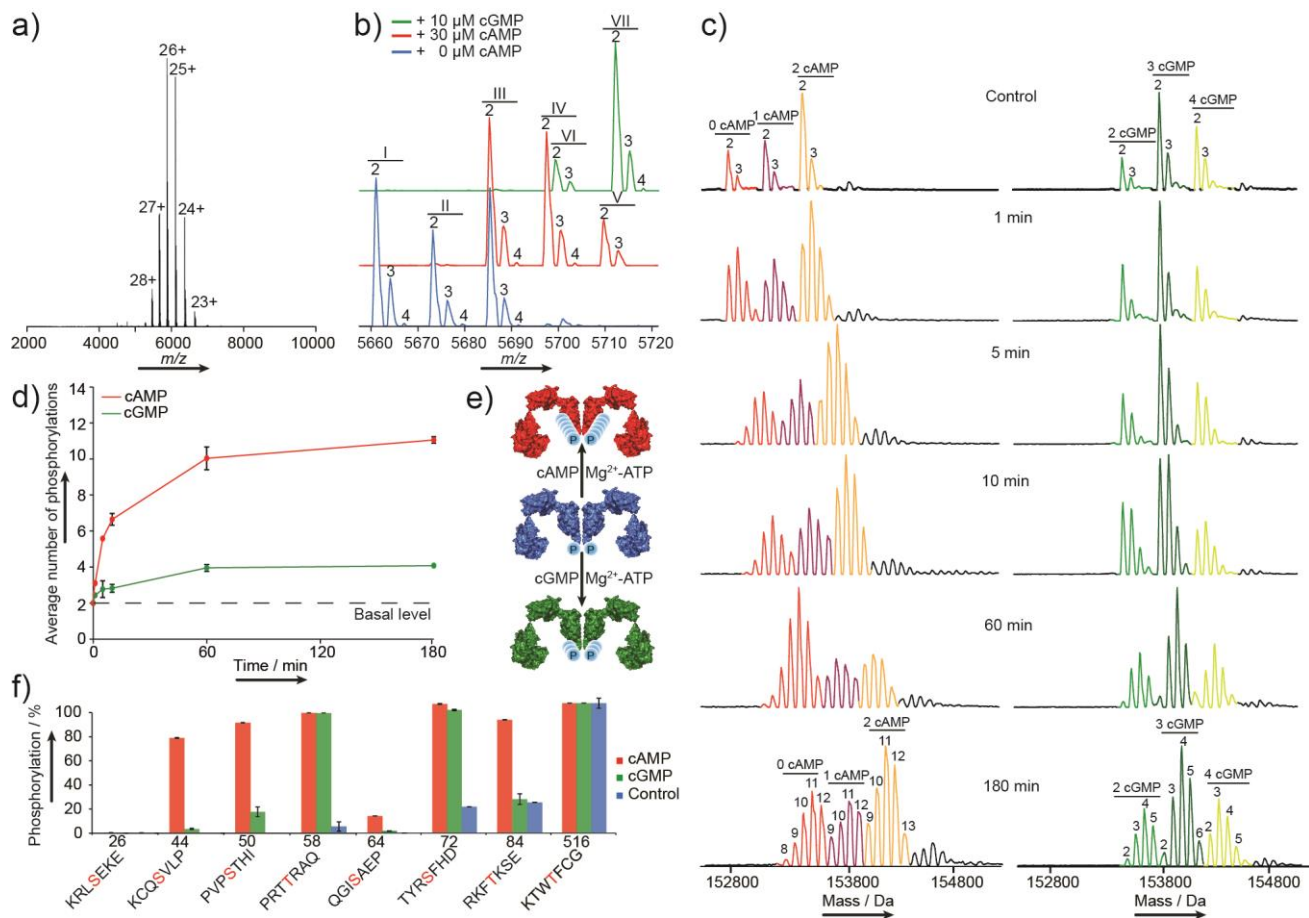


Figure 2. Comprehensive analysis of the cAMP (red) and cGMP (green) mediated auto-phosphorylation of PKG with native and bottom-up mass spectrometry. a) Broad range native mass spectrum of PKG. The main mass derived from this charge-state envelope is 152817.6 Da corresponding with the expected mass of dimeric PKG. b) Zoom in on the $[M+27H]^{27+}$ signal and the observed mass shifts upon addition of cAMP or cGMP. Arabic numerals indicate the number of attached phosphate groups per dimer, roman numerals indicate distinct cyclic nucleotide bound states. The spectrum in blue reveals that purified PKG has already 0-2 cAMP molecules bound (species I-III), and 2-4 phosphate groups incorporated. Following incubation with cyclic nucleotides, PKG binds 2-4 cAMP (species III-V) or 3-4 cGMP molecules (species VI-VII), respectively. c) Native mass spectra illustrating the progressive auto-phosphorylation of PKG upon incubation with Mg^{2+} -ATP and cAMP or cGMP. d) Changes of the intensity weighted average number of PKG auto-phosphorylations over time in the presence of cAMP or cGMP. After 180 minutes, PKG incubated with cAMP is phosphorylated on average 11 times, while PKG incubated with cGMP is phosphorylated on average 4 times. e) Schematic representation of the differential auto-phosphorylation of PKG in the presence of cAMP or cGMP. f) Identification and quantification of phosphorylated sites on PKG by bottom-up LC/MS-MS. In the presence of cAMP, 6 sites per PKG monomer show significant levels of phosphorylation whereas, in the presence of cGMP, 3 sites are highly phosphorylated. Error bars indicate the standard deviation.

same trend of progressive phosphorylation towards a saturation point (Figure 3d). Bora, thus, seems to fulfil a dual role as transiently bound substrate and stable interaction partner of Aurora kinase A, as previously hypothesized^[12b] (Figure 3f). In summary, by combining high-resolution native MS and bottom-up LC-MS/MS in one workflow, we are able to characterize enzymatic protein phosphorylation at the level of amino acid sequence modifications, relative reaction kinetics and structural transitions. Finally, we argue that the strategy presented here can be applied to any enzyme/(protein-)substrate system, providing a generic approach to obtain sequential, kinetic and structural information in parallel.

reaction (Figure 3d). Bora, thus, seems to fulfil a dual role as transiently bound substrate and stable interaction partner of Aurora kinase A, as previously hypothesized^[12b] (Figure 3f).

In summary, by combining high-resolution native MS and bottom-up LC-MS/MS in one workflow, we are able to characterize enzymatic protein phosphorylation at the level of amino acid sequence modifications, relative reaction kinetics and structural transitions. Finally, we argue that the strategy presented here can be applied to any enzyme/(protein-)substrate system, providing a generic approach to obtain sequential, kinetic and structural information in parallel.

Experimental Section

Kinase reactions were carried out under physiological pH in presence of ATP and magnesium chloride at 30°C with a 1000-fold molar excess of cAMP or cGMP (PKG) or at room temperature with a 2-fold excess of Bora (AurA).

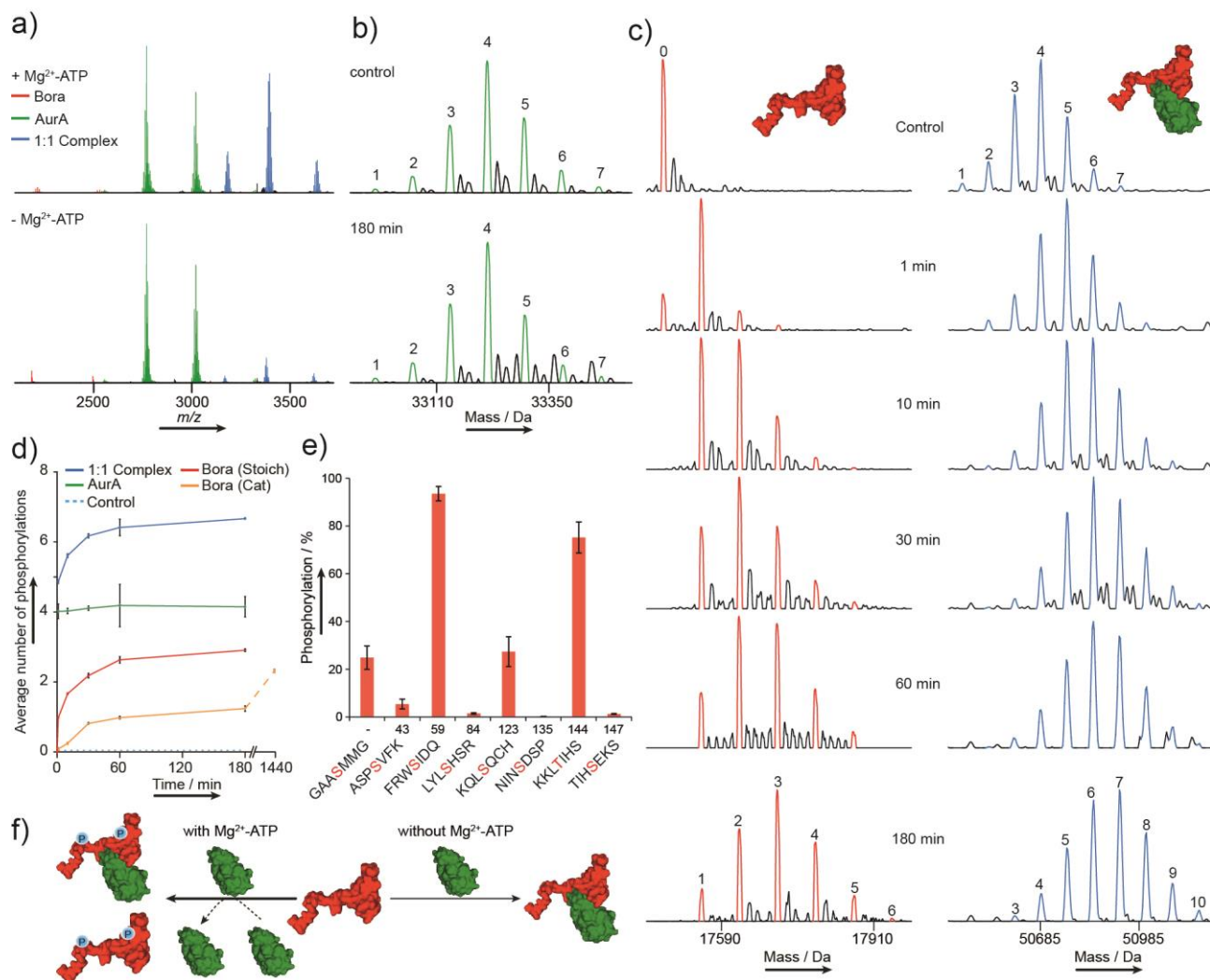


Figure 3. Comprehensive analysis of the interplay between the substrate Bora (red) and the kinase Aurora A (AurA, green) by native and bottom-up mass spectrometry. a) Native MS analysis of AurA (32.9 kDa) and Bora (17.5 kDa) reveals that, after 180 min incubation, the 1:1 complex (blue signals, 50.4 kDa) forms more efficiently with Mg^{2+} -ATP added. b) Purified AurA shows 7 distinct phospho-isoforms. Phosphorylation does not further increase upon incubation with Mg^{2+} -ATP. c) Native MS evidences the progressive phosphorylation of Bora and the AurA/Bora complex in presence of Mg^{2+} -ATP. Numerals above the peaks indicate the number of phosphorylations. d) Plotting the weighted average number of phosphorylations versus time shows that the phosphorylation of Bora and the complex increases towards a saturation point, when stoichiometric AurA/Bora ratios ('Stoich') are used. Adding near-catalytic amounts of AurA facilitates progressive Bora phosphorylation as well ('Cat', orange curve). e) Identification and quantification of phosphorylated sites on Bora by bottom-up LC/MS-MS. No phosphorylation was detected in the negative controls. The unnumbered phosphorylation site is not part of the Bora sequence in Uniprot KB. Error bars represent standard deviations. f) Model for the AurA/Bora interaction. AurA forms a stable complex with unphosphorylated Bora and, conversely, Bora phosphorylation proceeds already at catalytic AurA concentrations. Thus, complex formation and phosphorylation are likely to represent two independent modes of interaction.

Reaction quenching was performed on ice by adding EDTA. After buffer exchange to ammonium acetate pH 6.8, samples were analyzed using a modified Orbitrap Exactive Plus mass spectrometer, with settings optimized to obtain high resolution and sensitivity and kept constant for the specific proteins. For LC-MS/MS analysis, reaction mixes were denatured, reduced, alkylated and subsequently digested using trypsin and GluC (PKG) or trypsin (AurA/Bora). After desalting, samples were analyzed on a LTQ-Orbitrap Elite coupled to a Proxeon EASY-nLC 1000. Additional experimental details are available in the Supporting Information.

Received: ((will be filled in by the editorial staff))
Published online on ((will be filled in by the editorial staff))

Keywords: Analytical methods, Mass spectrometry, Protein modifications, Protein-protein interactions, Kinase assay

- [1] a) J. D. Scott, T. Pawson, *Science* **2009**, *326*, 1220-1224; b) T. Hunter, *Cell* **1995**, *80*, 225-236; c) T. Hunter, *Philos. Trans. R. Soc. Lond. B. Biol. Sci.* **2012**, *367*, 2513-2516.
[2] a) J. V. Olsen, M. Mann, *Mol. Cell. Proteomics* **2013**, *12*, 3444-3452; b) S. Lemeer, A. J. Heck, *Curr. Opin. Chem. Biol.* **2009**, *13*, 414-420.
[3] K. Brumbaugh, W. Johnson, W. C. Liao, M. S. Lin, J. P. Houchins, J. Cooper, S. Stoesz, R. Campos-Gonzalez, *Methods Mol. Biol.* **2011**, *717*, 3-43.
[4] P. A. Grimsrud, D. L. Swaney, C. D. Wenger, N. A. Beauchene, J. J. Coon, *ACS Chem. Biol.* **2010**, *5*, 105-119.

- [5] a) Y. Jia, C. M. Quinn, S. Kwak, R. V. Talanian, *Curr. Drug Discov. Technol.* **2008**, *5*, 59–69; b) C. Salazar, T. Hofer, *FEBS J.* **2009**, *276*, 3177–3198.
- [6] H. Nishi, K. Hashimoto, A. R. Panchenko, *Structure* **2011**, *19*, 1807–1815.
- [7] a) Y. L. Deribe, T. Pawson, I. Dikic, *Nat. Struct. Mol. Biol.* **2010**, *17*, 666–672; b) S. S. Taylor, R. Ilouz, P. Zhang, A. P. Kornev, *Nat. Rev. Mol. Cell Biol.* **2012**, *13*, 646–658.
- [8] a) J. Marcoux, C. V. Robinson, *Structure* **2013**, *21*, 1541–1550; b) M. Sharon, *Science* **2013**, *340*, 1059–1060; c) A. J. Heck, *Nat. Methods* **2008**, *5*, 927–933; d) J. A. Loo, *Mass Spectrom. Rev.* **1997**, *16*, 1–23.
- [9] R. J. Rose, E. Damoc, E. Denisov, A. Makarov, A. J. Heck, *Nat. Methods* **2012**, *9*, 1084–1086.
- [10] a) S. Rosati, R. J. Rose, N. J. Thompson, E. van Duijn, E. Damoc, E. Denisov, A. Makarov, A. J. Heck, *Angew. Chem.* **2012**, *124*, 13166–13170; b) S. Rosati, R. J. Rose, N. J. Thompson, E. van Duijn, E. Damoc, E. Denisov, A. Makarov, A. J. Heck, *Angew. Chem. Int. Ed. Engl.* **2012**, *51*, 12992–12996; c) S. Rosati, E. T. van den Bremer, J. Schuurman, P. W. Parren, J. P. Kamerling, A. J. Heck, *mAbs* **2013**, *5*, 917–924.
- [11] a) K. Takio, S. B. Smith, K. A. Walsh, E. G. Krebs, K. Titani, *J. Biol. Chem.* **1983**, *258*, 5531–5536; b) A. Aitken, B. A. Hemmings, F. Hofmann, *Biochim. Biophys. Acta* **1984**, *790*, 219–225; c) M. W. Pinkse, A. J. Heck, K. Rumpel, F. Pullen, *J. Am. Soc. Mass Spectrom.* **2004**, *15*, 1392–1399; d) M. W. Pinkse, P. M. Uitto, M. J. Hilhorst, B. Ooms, A. J. Heck, *Anal. Chem.* **2004**, *76*, 3935–3943.
- [12] a) A. Seki, J. A. Coppinger, C. Y. Jang, J. R. Yates, G. Fang, *Science* **2008**, *320*, 1655–1658; b) A. Hutterer, D. Berdnik, F. Wirtz-Peitz, M. Zigman, A. Schleiffer, J. A. Knoblich, *Dev. Cell* **2006**, *11*, 147–157; c) F. Eckerdt, J. L. Maller, *Trends Biochem. Sci.* **2008**, *33*, 511–513.
- [13] T. M. Lincoln, N. Dey, H. Sellak, *J. Appl. Physiol.* **2001**, *91*, 1421–1430.
- [14] M. Mann, C. K. Meng, J. B. Fenn, *Anal. Chem.* **1989**, *61*, 1702–1708.
- [15] H. Poppe, S. D. Rybalkin, H. Rehmann, T. R. Hinds, X. B. Tang, A. E. Christensen, F. Schwede, H. G. Genieser, J. L. Bos, S. O. Doskeland, J. A. Beavo, E. Butt, *Nat. Methods* **2008**, *5*, 277–278.
- [16] E. H. Y. Chan, A. Santamaria, H. H. W. Sillje, E. A. Nigg, *Chromosoma* **2008**, *117*, 457–469.
- [17] A. O. Walter, W. Seghezzi, W. Korver, J. Sheung, E. Lees, *Oncogene* **2000**, *19*, 4906–49016.
- [18] A. N. Kettenbach, D. K. Schweppe, B. K. Faherty, D. Pechenick, A. A. Pletnev, S. A. Gerber, *Sci. Signal.* **2011**, *4*, rs5.

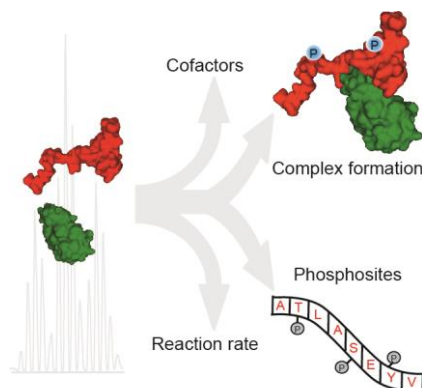
Entry for the Table of Contents

Layout 1:

Protein Mass Spectrometry

Michiel van de Waterbeemd, Philip Lössl, Violette Gautier, Fabio Marino, Masami Yamashita, Elena Conti, Arjen Scholten, Albert J.R. Heck
_____ **Page – Page**

Simultaneous Assessment of Kinetic, Site-Specific and Structural Aspects of Enzymatic Protein Phosphorylation



All-inclusive monitoring of protein phosphorylation. Phosphate incorporation is a universal modification of cellular proteins with multiple functional implications. By combining native and bottom-up MS we follow phosphorylation reactions over time, simultaneously visualizing dynamic non-covalent protein interactions, identifying phosphorylated amino acids, and quantifying all occurring phosphoisoforms to obtain kinetic data.